

Microstructure of a sintered 16.5 mol % CeO₂–ZrO₂ alloy at cryogenic temperature

LI LAI-FENG, HONG CHAO-SHENG, ZHANG ZHONG

Cryogenic Laboratory, Chinese Academy of Sciences, PO Box 2711, Beijing 100080, People's Republic of China

LI YI-YI

Institute of Metal Research, Chinese Academy of Sciences, Shenyang 110015, People's Republic of China

The microstructure of a fine grained 16.5 mol % CeO₂–stabilized tetragonal zirconia polycrystal (Ce-TZP) has been investigated by transmission electron microscopy observations. The results show that the samples fractured at 298, 77 and 4.2 K change significantly. At 298 K, there is no stress-induced martensite but a few anti-phase boundaries (APB) in the tetragonal (t) parent phase. With a decrease in testing temperature, monoclinic (m) product, or martensite within retained t phase, appears. Its morphologies are characterized as lenticular and block-like at 77 K and as lenticular and butterfly-like at 4.2 K. The relationship between microstructure and mechanical properties is also discussed.

1. Introduction

It is well established that zirconia-based ceramics have high strength and toughness due to the stress-induced metastable tetragonal (t) to monoclinic (m) transformation which is identified as diffusionless or martensitic in nature [1–3]. However, most of the studies on these material types are focused on the behaviours at room temperature or above. Since ceramics have many specific features, such as high rigidity, large ratio of strength: thermal conductivity and good size stability, they can be used as the optimal structural materials for cryogenic engineering. High strength and toughness of ZrO₂-based ceramics at the cryogenic temperature can be obtained by carefully controlling the CeO₂ content [4, 5]. To understand the mechanism of transformation-induced toughening at such a temperature requires detailed studies of the morphology of the transition product; however, little is known about the effects of chemical composition and heat treatment on morphology, and few research activities conduct cryogenic temperature mechanical properties.

The purpose of the present paper seeks to probe the relationship between microstructure and mechanical properties on 16.5 mol % Ce-TZP, which has excellent mechanical properties at the cryogenic temperature among compositions checked in our previous study [4].

2. Experimental procedure

The preparation of 16.5 mol % Ce-TZP and its mechanical property measurements are reported elsewhere [4].

The samples were prepared for transmission electron microscopy (TEM) examination using standard

techniques, i.e. diamond-watering thin slices, grinding and polishing to ca. 25 μm thickness, followed by ion-beam thinning to electron transparency. A thin C coat was sputtered on one surface before insertion into an EM-420 microscope.

X-ray diffraction (XRD) patterns were obtained using a Philips automatic diffractometer (model PW 1140) operating at 40 kV with CuK_α radiation and a graphite monochromator. The m phase content was obtained from integrated intensities of (1 1 1)_m, (1 1 $\bar{1}$)_m and (1 1 1)_t peaks using the method developed by Porter and Heuer [6].

Martensite start temperature (M_s) was measured using a strain-gauge technique in which a G-M refrigerator was employed.

3. Results and discussion

3.1. Mechanical properties of 16.5 mol % Ce-TZP

Table I shows the martensite content in the fractured surface, the bending strength and fracture toughness at various testing temperatures: M_s is 41.6 K.

It is seen from Table I, that there are dramatic increases in strength and toughness at 77 and 4.2 K. Moreover, martensite content increases with a decrease in testing temperature. The improvements of mechanical properties are due to stress-induced martensitic transformation at the ambient M_s . Strengthening and toughening are closely related to M_s ; if M_s is much higher than the testing temperature, the properties will drop significantly because most martensite arises from spontaneous transformation, not from stress-induced. Lower CeO₂ content TZP, such as 12 mol % CeO₂, has excellent mechanical properties

TABLE I Martensite content and mechanical properties for 16.5 mol % Ce-TZP

T (K)	Mol % (vol)	σ_b (MPa)	K_{Ic} (MPa m ^{1/2})
298	0	494.4	6.94
77	7.4	600.8	11.17
4.2	21.9	729.8	15.06

at ambient room temperature because its M_s is ca. 200 K. However, if the testing temperature is 73 K, which is much lower than its M_s , the mechanical properties rapidly reduce [7].

3.2. Morphologies of martensite

The dopant content change referring to a certain testing temperature affects not only the macro-mechanical properties but morphologies of martensite in t to m transformation. Previous studies on either Y-TZP or Ce-TZP at testing temperatures around room temperature, with comparatively low dopant content, showed almost unique plate-like martensite. However, our TEM observations show various morphologies of

16.5 mol % Ce-TZP at cryogenic testing temperatures (see Fig. 1). At 77 K, martensite occurs chiefly as lenticular and block-like (Fig. 1a and b); but at 4.2 K, as lenticular and butterfly-like (Fig. 1c and d).

We have also found an interesting phenomenon in the sample fractured at 77 K (see Fig. 2). A big tetragonal grain splits into several small grains, or subgrains, which are composed of dislocation networks. We believe that it may represent the critical state of t to m transition and may result in various martensite morphologies.

During the process of TEM observation, we noted that the amount of martensite at 4.2 K is much greater than that at 77 K, which is roughly consistent with the results obtained from XRD studies.

3.3. Anti-phase boundaries (APB) in the sample fractured at room temperature

Although no t to m transformation occurred at room temperature, we found some APB on fractured surfaces (see Fig. 3). As we know, in addition to t to m martensitic transformation in ZrO₂-based ceramics, the cubic (high temperature phase) to tetragonal (c to t) transformation is also identified as martensitic process

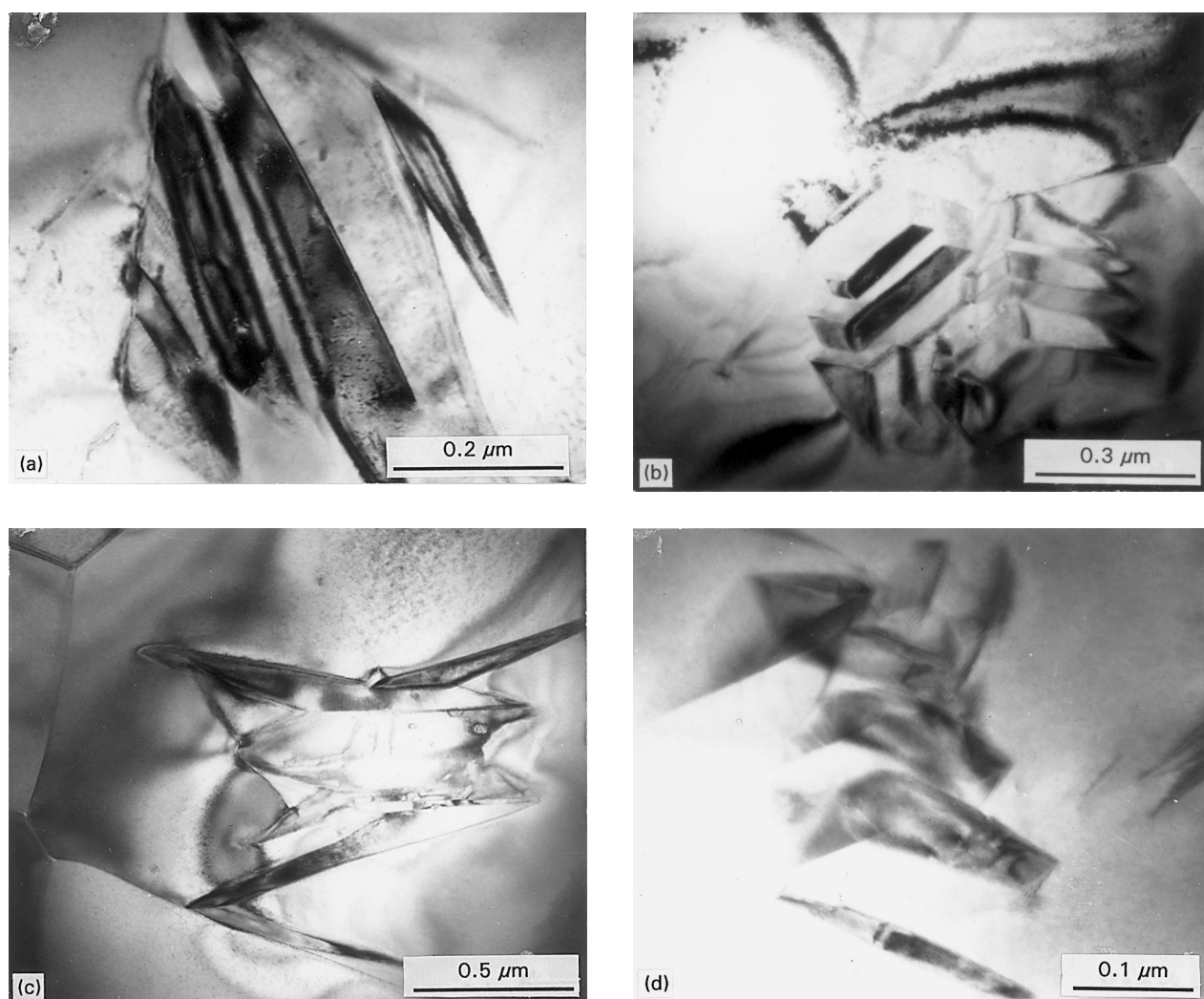


Figure 1 TEM micrographs of Ce-TZP containing m products within retained t phase. (a) Lenticular-like and (b) block-like in the sample fractured at 77 K; (c) lenticular-like and (d) butterfly-like in the sample fractured at 4.2 K.

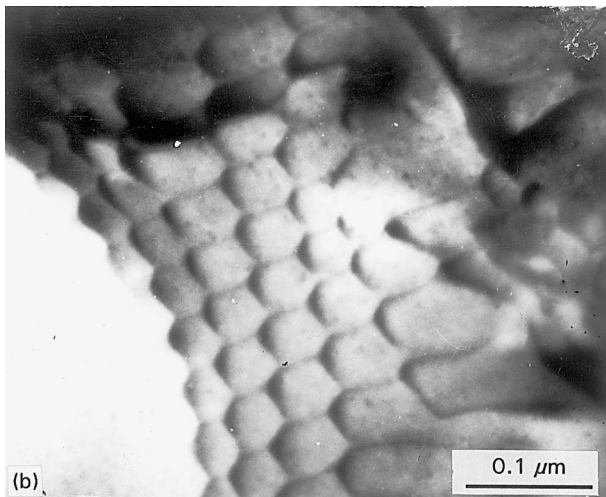
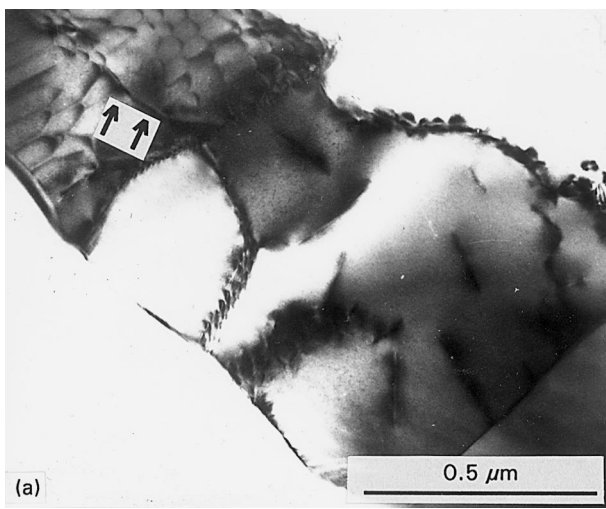


Figure 2 At phase grain composed of several dislocation networks (a) which may indicate the critical state of *t* to *m* transformation, and the enlargement image (b) of the arrowed zone in (a) which clearly shows a hexagonal dislocation net coming from the reaction of some partial dislocations.

[8]. The transition product is called the *t'* phase, which is crystallographically identical but morphologically different to the *t* phase. The *t'* phase has the feature of a herring-bone structure [9–12] and APB [12–14]. Unlike the *t* phase, it is quite resistant to *t'* to *m* transformation under stress, therefore it is ineffective for improving toughness [15]. The preparation of the *t'* phase requires heating the sample either in the range of cubic stability or above the melting point followed by rapid cooling [9, 13, 16]. Moreover, a high dopant content is also required. For Y_2O_3 – ZrO_2 systems, the Y_2O_3 content needs to be ≥ 3 mol% [9, 13]; for CeO_2 – ZrO_2 systems, the CeO_2 content needs to be ≥ 17 mol% [15]. These contents correspond to a *c* + *t* dural or a single *c* phase region in the diagrams. But studies for Y_2O_3 – ZrO_2 showed that the appearance of APB was just reliable in a narrow range of 4–7 mol% Y_2O_3 , and beyond this no APB were found [13, 14]. By checking their phase diagrams, we find that the composition range for APB is not far from the solubility limit of dopant in the *t* matrix and APB will derive from it during the cooling process. This view thus differs from that of other authors who

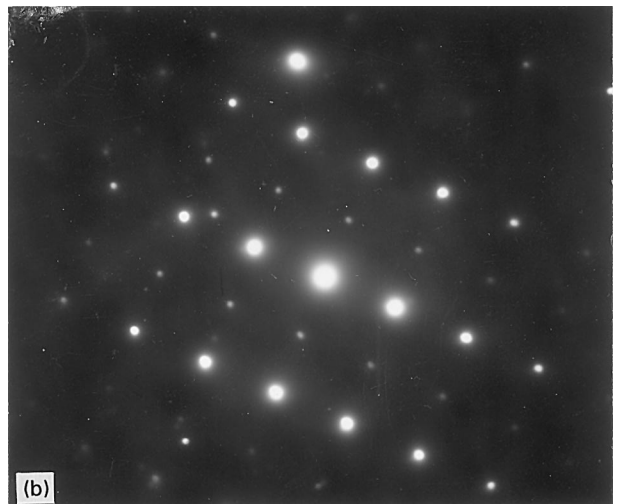
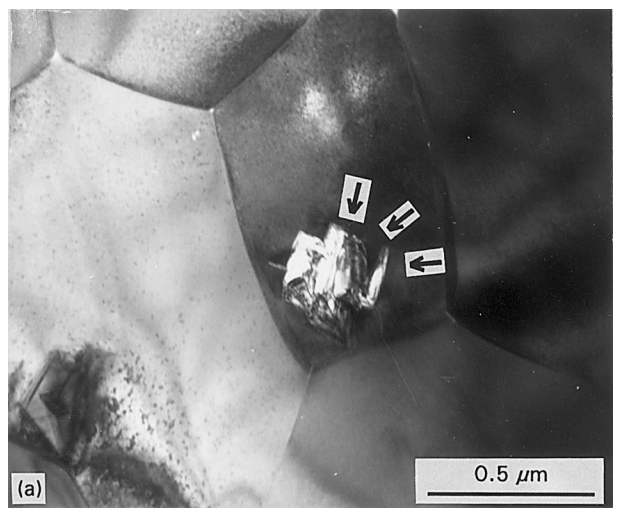


Figure 3 Anti-phase boundary (arrowed) (a) and [101] diffraction pattern (b) of the sample fractured at room temperature.

described the APB as the *t'* phase [12–14]. In fact, the *t'* phase retains its unique herring-bone feature no matter what the dopant content. It relates only to the sintering temperature and cooling rate. By melting or sintering at about 2100 °C (single cubic region), even low Y_2O_3 contents, such as 2 mol%, have a *c* to *t'* transition, and the *t'* phase is completely of a herring-bone structure, with no APB [17]. APB appear only at the compositions where the dopant contents are in the vicinity of the *t* and *c* phase boundary in the diagram. This can be explained from our experiment on 16.5 mol% Ce-TZP. It undergoes no *c* to *t'* transition because its sintering temperature is 1450 °C, where it is in the single *t* phase region, but APB are found. Through careful analysis of TEM diffraction, although the diffraction roughly accords with that of the *t'* phase, it more accurately agrees with that of $ZrCeO_4$ compound whose XRD card number is 38-1436. Therefore, the APB are superlattice $ZrCeO_4$ and not the *t'* phase.

4. Conclusions

We conclude that the improvements of cryogenic temperature mechanical properties for ZrO_2 –16.5 mol%

CeO₂ alloys are dependent on the microstructural evolution. APB appeared in samples fractured at room temperature and are the main strengthening agent. TEM reveals that the APB are superlattice ZrCeO₄ compounds rather than the t' phase.

Acknowledgements

The authors thank Jiang Ming for help with preparation of materials, and Gong Ling-Hui and Professor Zhang Liang for help with measurements of M_s .

References

1. G. K. BANSAL and A. H. HEUER, *Acta Metall.* **20** (1972) 1281.
2. E. C. SUBBARO, H. S. MAITI and K. K. SRIVASTAVA, *Phys Status Solidi A* **21** (1974) 9.
3. R. C. GARVIE, R. H. HANNINK and R. T. PASCOE, *Nature* **258** (1975) 703.
4. L. F. LI, Z. ZHANG, L. Z. ZHAO, Z. H. TU and Y. Y. LI in Proceedings the 15th International Cryogenic Engineering Conference, June (1994) (Genova, Italy, in press).
5. T. K. GUPTA and C. A. ANDERSON, *Adv Cryogenic Engng* **30** (1983) 367.
6. D. L. PORTER and A. H. HEUER, *J. Amer. Ceram. Soc.* **62** (1979) 2897.
7. M. HAYAKAWA, H. SHINMEN and M. OKA, in Proceedings of the International Conference on Martensitic Transformation, 1992 (Monterey Institute for Advanced Studies, Monterey, California, USA, 1993) p. 677.
8. C. A. ANDERSON Jr, GREGGI and T. K. GUPTA, in "Advances in Ceramics", Vol. 12, Science and Technology of Zirconia II, edited by (N. Classen *et al.* (The American Ceramic Soc., 1984) p. 78.
9. H. G. SCOTT, *J. Mater. Sci.* **10** (1975) 527.
10. R. CHAIM, M. RULE, A. H. HEUER, *J. Amer. Ceram. Soc.* **68** (1985) 427.
11. B. C. MUDDLE and G. R. HUGO, in Proceedings of the International Conference on Martensitic Transformation, 1992 (Monterey Institute for Advanced Studies, Monterey, California, USA, 1993) p. 647.
12. T. SAKUMA, Y. A. YOSHIZAWA and H. SATO, *J. Mater. Sci.* **20** (1985) 2399.
13. Y. ZHOU, T. C. LEI and S. SAKUMA, *J. Amer. Ceram. Soc.* **74** (1991) 633.
14. V. LANTERI, R. CHAIM and A. H. HEUER, *ibid.* **69** (1986) c-258.
15. S. MASCHIO, O. SBAIZERO and S. MERIANI, *J. Euro. Ceram. Soc.* **9** (1992) 127.
16. S. BHATTACHARJEE, U. SYMAPRASAD, R. K. GAGLI and B. C. MOHANTY, *Mater. Lett.* **15** (1992) 281.
17. M. HAYAKAWA, Y. ONDA and M. OKA, in Proceedings of the International Conference on Martensitic Transformation, 1992 (Monterey Institute for Advanced Studies, Monterey, California, USA, 1993) p. 707.

Received 12 October 1994
and accepted 13 February 1996